Aspergillus nidulans ambient pH signaling does not require endocytosis

Daniel Lucena-Agell[1], Antonio Galindo[2], Herbert N. Arst, Jr[1, 3] and Miguel A. Peñalva[1,#]

[1] Department of Cellular and Molecular Biology, Centro de Investigaciones Biológicas CSIC, Madrid, Spain; [2] Division of Cell Biology, MRC Laboratory of Molecular Biology, Cambridge, UK; [3] Section of Microbiology, Imperial College London, UK

Address correspondence to Miguel A. Peñalva, penalva@cib.csic.es

Running head: pH signaling does not require endocytosis

Summary

Aspergillus nidulans (Pal) ambient pH signaling takes place in cortical structures containing components of the ESCRT pathway, which are hijacked by the alkaline pH-activated, ubiquitin-modified version of the arrestin-like protein PalF to the plasma membrane. There ESCRTs scaffold the assembly of dedicated Pal proteins acting downstream. The molecular details of this pathway, which results in the two-step proteolytic processing of the transcription factor PacC, have received considerable attention due to the key role that it plays in fungal pathogenicity. While current evidence strongly indicates that the pH signaling role of ESCRT complexes is limited to plasma membrane-associated structures where PacC proteolysis would take place, the localization of the PalB protease which almost certainly catalyzes the first and only pH-regulated proteolytic step had not been investigated. In view of ESCRT participation, this leaves formally open the possibility that PalB activation requires endocytic internalization. As endocytosis is essential for hyphal growth, non-lethal endocytic mutations are predicted to cause an incomplete block. We used a SynA internalization assay to measure the extent at which any given mutation prevents endocytosis. We show that none of the tested mutations impairing endocytosis to different degrees, including *slaB1* conditionally causing a complete block, have any effect on the activation of the pathway. We further show that PalB, like PalA and PalC, localizes to cortical structures in alkaline pH dependent manner. Therefore signaling through the Pal pathway does not involve endocytosis.

Introduction

In *Aspergillus nidulans* the alkaline ambient pH-sensing plasma membrane module involves three proteins, the 7-transmembrane domain (TMD) receptor PalH, the arrestin-like PalF and the 3-TMD helper PalI (1-5). This sensing module transduces a signal generated by alkaline ambient pH to a downstream module containing the Snf7 interactors PalA and PalC and the signaling protease PalB (3, 6-11). The downstream module also involves components of endosomal sorting complexes required for transport (ESCRT)-I, ESCRT-II and Snf7 and Vps20 of ESCRT-III (10, 12). PalB, the final Pal participant in the pathway, almost certainly catalyzes the C-terminal proteolysis of the 72 kDa form of the transcription factor PacC (PacC72) to yield PacC53 and, following a second proteasome-mediated limited proteolysis, PacC27 (4, 13-15).

The pH signaling involvement of ESCRT complexes, which have a key role in multivesicular body (MVB) sorting in endosomes, led to a model in which the pH sensing module and the ESCRT-associated proteins would be spatially separated, with the former located at the plasma membrane and the latter located on the membrane of endosomes (16). The two complexes would be connected by endocytosis, such that the activated plasma membrane sensor would be sorted in endocytic vesicles that would traffic to endosomes to engage downstream components and ultimately activate PalB-mediated PacC72 proteolysis in this locale. This model was challenged when localization experiments demonstrated that rather than being recruited to endosomes, PalA and PalC were recruited to cortical plasma-membrane associated foci in an alkaline ambient pH- and ESCRT-dependent manner (8, 10). This and the observation that the key ESCRT-I component Vps23 was recruited to similar membrane-associated foci (10) strongly indicated that the PalH/PalF sensor module hijacks ESCRTs to the plasma membrane to scaffold pH signaling complexes. These data were also combined with evidence in both *A. nidulans* and *S. cerevisiae* showing that the toggle that triggers the signaling pathway is the PalH-dependent ubiquitination of PalF/Rim8 (2, 4, 17). Thus, in the revised and most recent model (5), PalH sensing of alkaline pH leads to ubiquitination of its PalF arrestin partner. PalF-Ub next recruits Vps23 to cortical spots and this results in the recruitment of ESCRT-II and the subsequent polymerization of ESCRT-III at cortical foci (10). This model also assumes that PalB, which is an ESCRT-III interactor (9), is recruited to these foci, implying that PacC72 cleavage takes place in them, which has not previously been demonstrated.

While it seems unquestionable that pH signaling complexes assemble on these foci, it cannot be ruled out that proteolysis requires endocytosis of the signaling complexes, a possibility circumstantially suggested by the case of mammalian arrestins, whose ubiquitination promotes

the endocytic internalization of their cognate receptors (18). Ambient pH-driven PalH internalization cannot be tested directly because PalH detection by GFP tagging requires overexpression, which artificially results in predominance of PalH in the endovacuolar system (3), rather than PalH localization in the plasma membrane.

Co-overexpression of PalI or PalF with overexpressed PalH-GFP prevents its localization to endovacuoles and results in plasma membrane predominance, strongly indicating that the sensing module must be assembled for its correct localization (3, 4). Thus, imaging whether PalH/PalF remains or not in the plasma membrane after exposure to alkaline pH would require overexpression of PalH, PalF and PalI, which may in turn make any downstream component limiting, casting doubts on any conclusion obtained with this experimental design.

A direct test of endocytic involvement in pH signaling would be to determine whether PacC72 processing proceeds in the absence of endocytosis. However, endocytosis is essential for *A. nidulans* because it plays a key role in hyphal growth (19-22), and thus the degree to which mutations preventing endocytosis permit hyphal growth is expected to correlate inversely with the extent to which they impair endocytosis, with a complete endocytic block being lethal (21-23). Here we demonstrate that PalB is also recruited to cortical structures. In addition, we make use of available mutations impairing endocytosis to show that none results in any detectable impairment in PacC72 proteolytic processing. Together these data strongly suggest that, in *A. nidulans*, endocytosis is not required for pH signaling.

Experimental Procedures

Strains

Unless otherwise indicated, *Aspergillus* complete (MCA) and synthetic complete medium (SC) (24), containing 1% glucose and, unless otherwise indicated, 5 mM ammonium tartrate (i. e. 10 mM NH_4^+) as carbon and nitrogen source, respectively, were used for growth tests and strain maintenance, except for the *slaB1* mutant, which was usually cultured on SC or MCA containing 10 mM nitrate. Strains, which carried markers in standard use, are listed in Table 1.

Microscopy

With the exception of PalB-GFP images, all other imaging was made using a Leica DMI6000 inverted microscope driven by Metamorph essentially as described (25, 26). Alkaline pH-mediated recruitment of PalB-GFP to cortical puncta was made as described for PalC-GFP (8), using a Nikon Eclipse E90 microscope, a Hamamatsu ORCA ER camera, a 1.4 N.A. 100 x objective and a Semrock Brightline-GFP filter combination. The set up was driven by Metamorph, which was used to manipulate all images. To determine the recruitment of PalB-GFP to cortical structures, cells were pre-cultured for 20 h at 25ºC in pH 5.2 (with 25 mM NaH_2PO_4) WMM (27) containing 1% ethanol (v/v) and 5 mM ammonium tartrate as carbon and nitrogen source, respectively. Germlings were shifted to acidic (pH 5.2) or alkaline (pH 8.2, with 25 mM Na_2HPO_4) medium and incubated for a further 30 min before being photographed. Cortical structures were counted in at least 32 germlings for each pH condition and the counts were normalized per micron of hyphal length. All images were converted to 8 bit and annotated with Corel Draw.

Constructs and genetic engineering

GFP-SynA transgenes have been described (25, 28, 29). For moderately high expression of PalH-GFP we used the constitutive $gpdA^{mini}$ promoter, contained within a pgpd003 construct that targets integration to the *pyroA* locus (30). Briefly, a chimera consisting of the PalH coding region with GFP attached in frame to its C-terminus was obtained from $pALC^{argB}$::PalH-GFP (our collection p1475) (12) and cloned as a HindIII-XmaI fragment in pgpd003, which was used for transformation into *A. nidulans* using pyridoxine prototrophy as selection. Single-copy transformants were identified by Southern blotting and used for all subsequent crosses. MAD1269 used to photograph PalB-GFP recruitment to cortical puncta carried a single copy integration (determined by Southern blotting) of p1398 into the *argB* locus. This plasmid consisted of a genomic copy of PalB with a C-terminal sGFP tag, expressed under the control of the $alcA^p$, and contains a frameshifted copy of *argB* targeting integration to the mutant *argB*2 allele of the recipient strain. This strain carried the null *palB38* allele such that *palB-GFP* was

137 the only source of PalB. Endogenously tagged *palB-GFP* was constructed by gene replacement
138 using a *palB-(GA)5-GFP::pyrG*^{Af}*::palB (3'-UTR)* cassette assembled by PCR.

139 **Cultures for pH shift experiments**

140 *A. nidulans* strains were cultured in 200 ml MM (inoculum, $3 \cdot 10^7$ conidiospores) containing 1%
141 glucose, 5 mM ammonium tartrate and appropriate supplements, adjusted to pH 4.3 with 50
142 mM sodium citrate. *slaB1* was cultured in MM containing 50 mM sodium nitrate or 25 mM of
143 ammonium sulphate (permissive and restrictive conditions, respectively). After 15 h incubation
144 at 30ºC under these acidic conditions, mycelia were collected by filtration using Miracloth
145 (Calbiochem) and transferred to fresh medium, buffered to pH 8 with HEPES-NaOH. Samples
146 were taken before and, at regular times, after the alkaline pH shift. Mycelia were pressed dry,
147 quick-frozen in dry ice and lyophilized to obtain 200-300 mg of dry weight per sample in the
148 case of strains showing relatively normal growth. A variation of this procedure was used for
149 *arfB*Δ, *fimA*Δ and *slaB*1 (ammonium conditions) owing to the low biomass yield. In these cases,
150 mycelia were collected by filtration using a 0.45 µm pore size filter. The yield of lyophilized
151 mycelia was 20-30 mg.

152 **Protein extraction and Western Blots**

153 This procedure was a modification of a reported protocol (22). Lyophilized mycelia were
154 homogenized using FP120 Fast Prep cell disruptor and a 0.5 mm ceramic bead, with a 10-s
155 pulse at a setting of 4.0. Aliquots (6 mg) of powdered biomass were transferred to a 2 ml
156 Eppendorf tube. Proteins were solubilized after addition of 1 ml of lysis solution (0.2 M NaOH
157 and 0.2% [vol/vol] β-mercaptoethanol) per tube and vigorous vortexing. Proteins were
158 recovered after precipitation with 7.5% (vol/vol) trichloroacetic acid (TCA) followed by
159 centrifugation at 14,000 *g* for 5 min at 4ºC. The resulting pellets were resuspended with 1 M
160 Tris Base (0.1 ml), mixed with 2 ml of Laemmli Buffer and incubated at 100ºC for 2 min.
161 Proteins (5 to 10 µl of each sample) were resolved in 8% SDS-polyacrylamide gels and electro-
162 transferred to nitrocellulose membranes. These were reacted either with mouse monoclonal anti-
163 c-myc (1/5000) (Clone 9E10 Sigma-Aldrich), rat monoclonal anti-HA (1/1000) (3F10, Roche)
164 or, for loading controls, mouse anti-actin monoclonal antibody (1/20000) (Clone 4, MP
165 Biomedicals, LLC) or rabbit anti-hexokinase polyclonal antibody (1/20000)(AB1807,
166 Chemicon International). Peroxidase-conjugated goat anti-rat IgM+G (3010-05, Southern
167 Biotech) at 1/4000, goat anti-mouse IgG immunoglobulin (Jackson) at 1/5000 (anti-Myc) or
168 1/8000 (anti-actin), and donkey anti-rabbit IgG (GE Healthcare, NA934) at 1/10000 were used
169 as appropriate. Peroxidase activity was detected with Amersham Biosciences ECL.
170

Results

SynA as a reporter of endocytosis

To assess the extent to which any given mutation impairs endocytosis we used a well-characterized cargo, the secretory v-SNARE SynA. SynA is an integral membrane protein of secretory carriers that are targeted to the apex by MyoE (31). Once SynA reaches the apical plasma membrane, it undergoes limited basipetal diffusion because it is very efficiently taken up by endocytosis mediated by a highly active ring of actin patches localized sub-apically. The combined action of targeted exocytosis and efficient endocytosis results in the typical steady-state localization of SynA to an apical crescent (21, 28) (Figure 1A).

Consistent with the fact that endocytosis prevents SynA diffusion across the plasma membrane (32), a double Val40Ala Met43Ala amino acid substitution in SynA preventing its endocytic sorting but having no effect on diffusion results in uniform SynA distribution along the plasma membrane (25, 33) (Figure 1B). Therefore, this uniform SynA distribution may be used to diagnose impairment of endocytosis. To validate further the diagnostic value of SynA localization, we photographed SynA in a strain carrying the $myoA^{S371E}$ mutation resulting in accelerated endocytosis (34). SynA was strongly polarized, more so than in the wild-type, consistent with its being taken up more rapidly after reaching the plasma membrane (Figure 1C). Thus, we conclude that SynA is a faithful and sensitive reporter of endocytosis.

Classification of *A. nidulans* endocytic mutations according to effectiveness

As endocytosis is essential, the extent to which a mutation impairs endocytosis was expected to correlate inversely with colony growth. The *A. nidulans* $sagA^{end3}$ gene encodes the *S. cerevisiae* End3 orthologue (35). A $sagA^{end3}$ null mutant displays a minor colony growth defect (Figure 2A), indicating that $sagA^{end3}$ is not crucial for endocytosis. Indeed SynA is still polarized in this mutant background. However, both in germlings and in long *sagA* Δ hyphae SynA localizes to the plasma membrane of tip-distal regions clearly more than in the wild-type, demonstrating that the mutation leads to an endocytic deficit, albeit minor (Figure 2A). ArfB and FimA are the *A. nidulans* orthologues of yeast Arf3 (36) and Sac6 (37), respectively. As judged by the severe defects in morphogenesis (19, 20) and colony growth (Figure 2B) displayed by the corresponding null mutants, these proteins were expected to be crucial for endocytosis. By microscopy, both *arfB*Δ and *fimA*Δ spores gave rise to heterogeneous cell populations (19, 20), some germlings showing yeast-like morphology and some cells progressing to hyphae, in many cases morphologically aberrant. In both cases SynA was depolarized, indicating a major endocytic deficit (Figure 2B).

slaB is the *A. nidulans* orthologue of *S. cerevisiae SLA2*, a key regulator of endocytic patches (38, 39). We have previously demonstrated using heterokaryon rescue that *slaB* deletion is lethal (21), a conclusion that was further buttressed using *slaB1*, a conditional expression allele having the *niiA* (encoding nitrite reductase) promoter, which is repressible by ammonium and inducible by nitrate (22) (Figure 2C). On ammonium, *slaB1* spores germinate but do not maintain polarity beyond yeast-like cells and do not internalize SynA, forming characteristic pits in the plasma membrane (Figure 2C) (22). Contrary to the heterogeneous populations observed with *arfB*Δ and *fimA*Δ strains, *slaB1* yeast-like cells represented the sole cellular type found under ammonium conditions. Altogether these data indicate that *sagA*Δ results in weak impairment of endocytosis, *arfB*Δ and *fimA*Δ result in stronger impairment, and *slaB1* (in ammonium conditions) essentially abolishes endocytosis

PalH has a tendency to be endocytosed if not stabilized in the plasma membrane

To confirm that mutations preventing SynA endocytosis have similar effects on the ambient pH receptor PalH we crossed transgenes encoding PalH-GFP into the mutant backgrounds. Figure 3A shows that, when overexpressed alone, PalH-GFP predominates in internal structures corresponding to endosomes and vacuoles, staining the plasma membrane only very faintly. Endocytosis is crucially dependent on F-actin polymerization (40). The subcellular distribution of PalH-GFP was markedly shifted towards the plasma membrane after treating cells with a sub-lethal concentration of the anti-F-actin drug latrunculin B to impair endocytosis (data not shown). Therefore, when overexpressed alone, PalH-GFP reaches the plasma membrane but has a strong tendency to be endocytosed.

Next we determined the effects of the different endocytosis mutations on PalH-GFP. These strictly correlated with those observed with SynA. *sagA*Δ weakly increased the localization of PalH to the plasma membrane (Figure 3B). *fimA*Δ and *arfB*Δ showed a similar, markedly stronger effect. In *fimA*Δ and *arfB*Δ, in both hyphae and abnormal 'giant' (yeast-like) cells, PalH largely predominated and exclusively localized, respectively, to the plasma membrane (Figure 3C), which incidentally suggests that hyphae progress beyond the stage of giant cells because although strongly impaired, they are incompletely blocked in endocytosis.

Endocytosis mutations do not prevent pH signaling

Having determined the degree to which the above mutations prevent PalH endocytosis, we examined, by western blots, the proteolytic processing of PacC in the different mutant backgrounds following a shift from acidic to alkaline conditions. We focused our analysis on the initial 30 min period after the pH shift, when PacC72 is converted to PacC53 by pH-dependent proteolysis, which is the readout of the activation of the Pal pathway (15) (Figures 4

and 5); [At the 30 min time point processing of PacC53 to PacC27 is also visible, but this second proteolysis step is pH-independent (14, 41, 42)].

The highly reproducible proteolytic processing activation pattern of PacC72 to PacC53 and PacC27 in wild-type cells shifted to alkaline conditions is displayed on the left panels of Figure 4. PacC processing patterns of the different mutants are shown on the right. Accelerated endocytosis due to *myoA*^{S371E} did not promote pH signaling (Figure 4A). Neither weak endocytosis-impairing *sagA*Δ nor the stronger endocytosis-impairers *arfB*Δ and *fimA*Δ substantially altered proteolytic PacC activation either (Figure 4B, C and D). These data, although strongly suggesting that endocytosis is not required for signaling, left open the possibility that residual endocytosis that in all likelihood takes place in *arfB*Δ or *fimA*Δ might suffice to enable pH signaling.

To eliminate this possibility we used *slaB1*. In *slaB1* cells cultured on nitrate, the distribution of (overexpressed) PalH-GFP was essentially indistinguishable from the wild-type, predominating very strongly in the endosomal system and localizing weakly to hyphal tips, a localization that was more conspicuous in young branches (Figure 5A). As noted above, *slaB1* cells on ammonium showed a uniform phenotype, with the population entirely consisting of yeast-like giant cells. These cells contained PalH localizing exclusively to the plasma membrane and associated endocytic pits (Figure 5B). Strong SlaB down-regulation in *slaB1* cells cultured in ammonium conditions, both at acidic pH and after shifting cells to alkaline pH, was confirmed by Western blots (Figure 5C). In these, SlaB was almost undetectable compared to the wild type control (note that SlaB was only detected when western blots were deliberately overexposed) (Figure 5C, middle). Thus, we proceeded to analyze pH signaling in *slaB1* cells cultured on ammonium (Figure 5D). Despite strong SlaB down-regulation PacC processing in response to alkaline pH was essentially normal (Figure 5D). Cells cultured in nitrate-containing medium, which results in strong SlaB up-regulation showed no effect either (Figure 5D).

In summary, none of the four different alleles impairing endocytosis to different degrees, including *slaB1* apparently resulting in a complete endocytic block, affect the PacC proteolytic cascade to any detectable extent, strongly indicating that endocytosis is not required at all for pH signaling.

PalB foci at the plasma membrane

A prediction derived from the fact that recruitment of the signaling protease PalB to ESCRTs is required for pH signaling (9), made in the context of ESCRT recruitment to plasma membrane-associated puncta, is that at alkaline pH PalB should also localize to cortical structures if

281 endocytosis were not required. Thus we tagged *palB* by gene replacement. We confirmed that
282 *palB::gfp* is functional by showing that strains carrying this allele behave as the wild-type in
283 diagnostic tests for pH regulation (Figure 6A). However, the signal of endogenously tagged
284 PalB-GFP was insufficient for microscopic analyses and indeed western blotting demonstrated
285 that levels of PalB-GFP were markedly lower than those of endogenously tagged PalA-GFP,
286 previously used to visualize cortical pH signaling structures (10) (Figure 6B) (In passing, this is
287 consistent with the catalytic role attributed to PalB). To circumvent this, we expressed PalB
288 under the control of the alcohol dehydrogenase gene promoter ($alcA^p$), and compared ethanol-
289 grown cells shifted to acidic and alkaline conditions by epifluorescence microscopy. These
290 experiments showed that PalB-GFP localized to cortical structures in alkaline pH-dependent
291 manner (Figure 6C).
292

293 ## Discussion

294

295 Previously we proposed a comprehensive model for pH regulation in which signal transduction
296 takes place in plasma membrane-associated foci scaffolded by ESCRT-III polymer (10). Strong
297 supporting evidence came from the findings that, in cells exposed to alkaline environment,
298 ESCRT subunits and late-acting pH signaling proteins PalC and PalA are recurrently recruited
299 to plasma membrane-associated foci (10), with down-regulation of ESCRT-disassembling Vps4
300 ATPase stabilizing PalC at these locales, indicating that recurrence at the plasma membrane
301 reflects ESCRT-III polymerization/depolymerization cycles (10). Evidence strongly indicates
302 that ubiquitination of the pH signaling arrestin-like protein PalF/Rim8 crucially regulates signal
303 transduction: the alkaline pH-dependent ubiquitin attachment to the arrestin docks ESCRT-I
304 Vps23 to receptor-arrestin complexes to organize subsequent ESCRT polymerizing steps at foci
305 (2, 4, 10, 17). A recent report using *S. cerevisiae* essentially concurred with the above
306 conclusions (43).
307

308 Two important predictions derive from the above model. One is the cortical localization of pH
309 signaling proteolysis. Indisputable evidence showed that PalB (9) and Rim13 (44) associate
310 with ESCRT-III, and that this association is required for signaling. Thus, PalB, like ESCRTs,
311 should be recruited to cortical foci in alkaline pH-dependent manner to mediate PacC
312 proteolysis. Indeed the Mitchell lab (44) demonstrated that *S. cerevisiae* Rim13 is recruited to
313 foci when cells encounter alkaline pH whereas others showed that these foci are actually
314 cortical (43). Here we report that PalB, like its yeast orthologue, is also recruited to cortical foci,
315 further supporting the contention that the 'plasma membrane' model applies to distant
316 ascomycete clades, in spite of the existence of minor differences in mechanistic detail between

317 *A. nidulans* and *S. cerevisiae* [for example PalB contains a MIT domain that contributes to its
318 recruitment to ESCRT-III (9) that is absent from Rim13]
319
320 If so, endocytosis should be dispensable for signaling. In yeast, endocytosis involves >30
321 proteins that are recruited in an orderly fashion to endocytic sites to mediate sequentially
322 clathrin coat assembly, cargo selection, membrane bending, actin polymerization and membrane
323 scission (38, 45). It has been reported that ablation of the early endocytic factor End3 (46), or
324 down-regulation of Las17 (47) does not prevent pH signaling in yeast (43), which was taken as
325 evidence against endocytosis involvement. However, the extent to these genetic manipulations
326 impair endocytosis was determined by FM4-64 uptake (thus bulk membrane internalization),
327 and this only qualitatively, leaving open the possibility that they impair, yet do not block all
328 endocytosis. End3 acts with clathrin, Sla1 (48), Sla2 (49) and Pan1 (50) in the coat assembly
329 step (38, 45). Indeed in a quantitative analysis of 400 viable null endocytosis-impairing
330 mutations (51), *end3*Δ ranked 315th (the greatest impairment being 1st), whereas *sla1*Δ ranked at
331 position 12th and *pan1*Δ and *sla2*Δ could not be ranked as they are lethal in the tested genetic
332 backgrounds. Similarly down-regulation of Las17, a regulator of actin polymerization, may be
333 insufficient to block all endocytosis, thus leaving open the possibility that basal levels suffice to
334 sustain pH signaling, should this involve endocytosis.
335
336 To address this issue we exploited the limited set of endocytosis mutations available in *A.*
337 *nidulans* (23), taking advantage of two phenotypic features to estimate their degree of endocytic
338 impairment. One was the extent to which any given mutation affects colony growth, a very
339 sensitive criterion because endocytosis is essential for hyphal growth (21, 22). Second, similarly
340 to the study by Burston et al. (51) in yeast, we took advantage of the fact that the synaptobrevin
341 SynA, like its yeast Snc1 orthologue (32, 33), is efficiently taken up by endocytosis and rapidly
342 recycled to the apex exocytically (25, 28, 29). This enables use of uniform plasma membrane
343 SynA distribution as a diagnostic of endocytic impairment. According to both criteria, *sagA*Δ
344 impaired endocytosis very weakly; *arfB*Δ and *fimA*Δ, which are phenotypically similar to each
345 other, prevented endocytosis substantially, even though they gave rise to heterogeneous
346 populations; finally, we used the regulatable *slaB1* allele and ammonium growth, which
347 completely prevented hyphal growth and SynA or PalH endocytosis. The absence of any
348 detectable effect in sensitive PacC proteolytic processing assays by any mutation included in
349 this panel represents strong evidence that pH signaling does not require endocytosis.
350
351 The alkaline pH signal received by PalH is decoded by the PalF arrestin-like protein (Rim8 in *S.*
352 *cerevisiae*). Fungal arrestins generally act as ubiquitin ligase adaptors that mediate
353 ubiquitination of their cognate plasma membrane protein partners, thus promoting their

endocytic- and MVB pathway-mediated down-regulation (52-56). In contrast, rather than promoting PalH internalization, PalF stabilizes PalH at the plasma membrane (4) and PalF/Rim8 ubiquitination plays a crucial, positive-acting role in pH signaling by recruiting ESCRTs to cortical sites (4, 10, 17). If this ESCRT recruitment occurred on endosomes, ubiquitinated PalF/Rim8 would inevitably be sorted for MVB degradation. Thus a highly speculative interpretation is that PalF-mediated recruitment of ESCRTs to the plasma membrane evolved as a mechanism by which pH signaling proteins exploit the scaffolding potential of ESCRT-III polymers without facing the threat of destruction.

Acknowledgements

We are very grateful to Greg May for *myoA*^{S371E}, to Brian Shaw for *arfB*Δ and *fimA*Δ, to Giorgos Diallinas for *sagA*Δ and to José M. Rodríguez for constructing, in the initial stages of this project, the p1398 plasmid and the transformed strain expressing PalB-GFP. Elena Reoyo provided excellent technical assistance. This work was supported by Ministerio de Economía y Competitividad (Spain) Grants BIO2009-07281 and BIO2012-30965 and by the Comunidad de Madrid (grant S2010/BMD2414). Daniel Lucena-Agell was holder of a FPI fellowship.

Figure legends

Figure 1. SynA as a reporter of endocytosis

(A) SynA is a single-pass v-SNARE delivered to the apex by exocytic carriers. Upon reaching to the plasma membrane it undergoes basipetal diffusion until captured by the sub-apical ring of endocytic patches (red circles), which acts as a diffusion barrier. (B) $SynA^{en-}$ is not taken up by endocytosis and therefore labels the plasma membrane uniformly (25). (C) In $myoA^{S371E}$ endocytosis is accelerated (34).

Figure 2. Growth and SynA localization phenotypes of endocytosis mutants

(A) Growth tests (at 37ºC) and GFP-SynA localization - in germlings and hyphae- in the *sagA*Δ mutant compared to the wild-type. (B) Growth phenotypes and SynA localization in *fimA*Δ and *arfB*Δ strains. (C) Growth and SynA localization phenotypes of *slaB1* cells (22) cultured on ammonium (20 mM ammonium sulfate) or nitrate (10 mM sodium nitrate), which are strongly repressing and inducing conditions, respectively, for the $niiA^{p}$-driven expression of SlaB. All microcopy images are displayed at the same magnification to facilitate inter-panel comparisons.

Figure 3. Effect of endocytosis-impairing mutations on the localization of PalH-GFP

(A) Wild-type strain carrying a single copy integration of a transgene driving expression of PalH-GFP under the control of the moderately strong $gpdA^{mini}$ promoter (30). The boxed inset is shown at double magnification to illustrate better the faint GFP staining of the plasma membrane. Internal structures are endosomes and vacuoles. (B) *sagA*Δ expressing PalH-GFP; note the faint yet consistently greater staining of the plasma membrane compared to the wild-type control. (C) *arfB*Δ expressing PalH-GFP. Note the heterogeneous population consisting of cells with strong and moderate labeling of the plasma membrane, in both cases uniformly. The boxed hypha shows a cell of the moderate labeling and 'more hyphal' class. (D) *fimA*Δ expressing PalH-GFP. Note the heterogeneous population as in the *arfB*Δ case. Fields in (C) and (D) are shown at half the magnification of those in (A) and (B) to illustrate population heterogeneity. As the $gpdA^{mini}$::*palH-gfp* transgene was in all cases a single-copy integration of the construct targeted to the *pyroA* locus, levels of PalH-GFP expression are in all cases equivalent.

Figure 4. Proteolytic processing activation of PacC in null endocytic mutants

Wild-type and mutant cells expressing wild-type Myc-PacC72 from the gene replacement allele *pacC900* were pre-cultured in acidic conditions and shifted to alkaline conditions for the indicated times. Cells were collected and analyzed by western blotting with anti-Myc antibody.

Anti-hexokinase (hxk) was used as loading control. (A) Wt *vs.* *myoA*^{S371A}cells. (B) Wt *vs.* *sagA*Δ cells. (C) Wt *vs.* *fimA*Δ cells. (D) Wt *vs.* *arfB*Δ cells.

Figure 5. On ammonium, *slaB1* completely prevents PalH endocytosis but does not alter the proteolytic processing activation of PacC

(A) *slaB1* hyphae cultured on nitrate, expressing PalH-GFP as in Fig. 3 legend. Left, note the localization to the plasma membrane at the nascent branch and the predominance in the vacuoles (indicated with 'v' letters). Right, hyphal tip cells showing weak plasma membrane staining (arrows) and basal conidiospores showing large and conspicuously fluorescent vacuoles. (B) A large field at the same magnification as those in (A) showing the homogeneus population of yeast-like cells resulting from cultivating the *slaB1* mutant on ammonium. The PalH-GFP puncta noticeable at the plasma membrane are large pits (not shown). (C) Western blot analysis of SlaB in *slaB1* cells cultured on ammonium and shifted from acidic to alkaline pH. The anti-SlaB western blots in the top and middle panels represent two different exposures for the same experiment. The lower panel is an anti-hexokinase (hxk) loading control. The middle panel was deliberately overexposed to reveal traces of SlaB (D) Normal proteolytic processing activation of PacC in *slaB1* cells, cultured on ammonium or nitrate, compared to the wild-type. As in (C), the anti-SlaB blot was deliberately overexposed to illustrate the extent of down-regulation. Nitrate conditions result in marked overexpression of SlaB. Hxk is hexokinase.

Figure 6. PalB is recruited to cortical puncta in an alkaline-dependent manner

(A) Diagnostic tests of pH regulation for *palB-GFP*. The null *palB*38 mutation prevents growth at pH 8.3 or on 0.3 M LiCl-containing media, leads to hyper-sensitivity to 10 mM sodium molybdate and to resistance to 1 mg/ml of neomycin. A *palB-GFP* gene replacement strain grows like the wild type at pH 8.3 and on LiCl and sodium molybdate plates and is as sensitive as the wild-type to neomycin, indicating that tagging does not impair function. (B) Western blot analysis of cells expressing endogenously tagged PalA-GFP or PalB-GFP. Actin is a loading control. (C) Cells expressing PalB-GFP under the control of the *alcA*^{p} were cultured on ethanol medium at acidic pH and shifted to acidic (H^+, 5.2) or alkaline (OH^-, 8.2) pH for 30 min before being photographed. The right diagram is a quantitation of the number of cortical structures per micron counted in n=32 hyphal tip cells cultured under acidic or alkaline conditions. Error bars are SE. The two sets of measurements are significantly different ($p < 0.001$) as determined with the Mann–Whitney *U* test.

References

1. **Negrete-Urtasun S, Reiter W, Díez E, Denison SH, Tilburn J, Espeso EA, Peñalva MA, Arst HN, Jr.** 1999. Ambient pH signal transduction in *Aspergillus* : completion of gene characterization. Mol Microbiol **33:**994-1003.

2. **Herranz S, Rodríguez JM, Bussink HJ, Sánchez-Ferrero JC, Arst HN, Jr., Peñalva MA, Vincent O.** 2005. Arrestin-related proteins mediate pH signaling in fungi. Proc Natl Acad Sci USA **102:**12141-12146.

3. **Calcagno-Pizarelli AM, Negrete-Urtasun S, Denison SH, Rudnicka JD, Bussink HJ, Munera-Huertas T, Stanton L, Hervás-Aguilar A, Espeso EA, Tilburn J, Arst HN, Jr., Peñalva MA.** 2007. Establishment of the ambient pH signaling complex in *Aspergillus nidulans* : PalI assists plasma membrane localization of PalH. Eukaryot Cell **6:**2365-2375.

4. **Hervás-Aguilar A, Galindo A, Peñalva MA.** 2010. Receptor-independent ambient pH signaling by ubiquitin attachment to fungal arrestin-like PalF. J Biol Chem **285:**18095-18102.

5. **Peñalva MA, Lucena-Agell D, Arst HN, Jr.** 2014. *Liaison alcaline*: Pals entice non-endosomal ESCRTs to the plasma membrane for pH signaling. Curr Opin Microbiol **22:**49-59.

6. **Negrete-Urtasun S, Denison SH, Arst HN, Jr.** 1997. Characterization of the pH signal transduction pathway gene palA of *Aspergillus nidulans* and identification of possible homologs. J Bacteriol **179:**1832-1835.

7. **Vincent O, Rainbow L, Tilburn J, Arst HN, Jr., Peñalva MA.** 2003. YPXL/I is a protein interaction motif recognised by *Aspergillus* PalA and its human homologue AIP1/Alix. Mol Cell Biol **23:**1647-1655.

8. **Galindo A, Hervás-Aguilar A, Rodríguez-Galán O, Vincent O, Arst HN, Jr., Tilburn J, Peñalva MA.** 2007. PalC, one of two Bro1 domain proteins in the fungal pH signaling pathway, localizes to cortical structures and binds Vps32. Traffic **8:**1346-1364.

9. **Rodríguez-Galán O, Galindo A, Hervás-Aguilar A, Arst HN, Jr., Peñalva MA.** 2009. Physiological involvement in pH signalling of Vps24-mediated recruitment of *Aspergillus* PalB cysteine protease to ESCRT-III. J Biol Chem **284:**4404-4412.

10. **Galindo A, Calcagno-Pizarelli AM, Arst HN, Jr., Peñalva MA.** 2012. An ordered pathway for the assembly of ESCRT-containing fungal ambient pH signalling complexes at the plasma membrane. J Cell Sci **125:**1784-1795.

11. **Denison SH, Orejas M, Arst HN, Jr.** 1995. Signaling of ambient pH in *Aspergillus* involves a cysteine protease. J Biol Chem **270:**28519-28522.

12. **Calcagno-Pizarelli AM, Hervás-Aguilar A, Galindo A, Abenza JF, Peñalva MA, Arst HN, Jr.** 2011. Rescue of *Aspergillus nidulans* severely debilitating null mutations in ESCRT-0, I, II and III genes by inactivation of a salt-tolerance pathway allows examination of ESCRT gene roles in pH signalling. J Cell Sci **124:**1-13.

13. **Espeso EA, Roncal T, Díez E, Rainbow L, Bignell E, Álvaro J, Suárez T, Denison SH, Tilburn J, Arst HN, Jr., Peñalva MA.** 2000. On how a transcription factor can avoid its proteolytic activation in the absence of signal transduction. EMBO J **19:**719-728.

14. **Díez E, Álvaro J, Espeso EA, Rainbow L, Suárez T, Tilburn J, Arst HN, Jr., Peñalva MA.** 2002. Activation of the *Aspergillus* PacC zinc-finger transcription factor requires two proteolytic steps EMBO J **21** 1350-1359.

15. **Peñas MM, Hervás-Aguilar A, Múnera-Huertas T, Reoyo E, Peñalva MA, Arst HN, Jr., Tilburn J.** 2007. Further characterization of the signaling proteolysis step in the *Aspergillus nidulans* pH signal transduction pathway. Eukaryot Cell **6** 960-970.

16. **Peñalva MA, Tilburn J, Bignell E, Arst HN, Jr.** 2008. Ambient pH gene regulation in fungi: making connections. Trends Microbiol. **16:**291-300.

17. **Herrador A, Herranz S, Lara D, Vincent O.** 2009. Recruitment of the ESCRT machinery to a putative seven-transmembrane-domain receptor is mediated by an arrestin-related protein. Mol Cell Biol **30:**897-907.

18. **Lefkowitz RJ, Shenoy SK.** 2005. Transduction of receptor signals by beta-arrestins. Science **308:**512-517.

19. **Upadhyay S, Shaw BD.** 2008. The role of actin, fimbrin and endocytosis in growth of hyphae in *Aspergillus nidulans*. Mol Microbiol **68:**690-705.

20. **Lee SC, Schmidtke SN, Dangott LJ, Shaw BD.** 2008. *Aspergillus nidulans* ArfB plays a role in endocytosis and polarized growth. Eukaryot Cell **7:**1278-1288.

21. **Araujo-Bazán L, Peñalva MA, Espeso EA.** 2008. Preferential localization of the endocytic internalization machinery to hyphal tips underlies polarization of the actin cytoskeleton in *Aspergillus nidulans*. Mol Microbiol **67:**891-905.

22. **Hervás-Aguilar A, Peñalva MA.** 2010. Endocytic machinery protein SlaB is dispensable for polarity establishment but necessary for polarity maintenance in hyphal tip cells of *Aspergillus nidulans.* Eukaryot Cell **9:**1504-1518.

23. **Peñalva MA.** 2010. Endocytosis in filamentous fungi: Cinderella gets her reward. Curr Opin Microbiol **13:**684-689.

24. **Cove DJ.** 1966. The induction and repression of nitrate reductase in the fungus *Aspergillus nidulans.* Biochimica and Biophysica Acta **113:**51-56.

25. **Pantazopoulou A, Peñalva MA.** 2011. Characterization of *Aspergillus nidulans* $RabC^{Rab6}$. Traffic **12:**386-406.

26. **Hernández-González M, Peñalva MA, Pantazopoulou A.** 2014. Conditional inactivation of *Aspergillus nidulans sarA* uncovers the morphogenetic potential of regulating endoplasmic reticulum (ER) exit. Mol Microbiol **95:**491-508.

27. **Peñalva MA.** 2005. Tracing the endocytic pathway of *Aspergillus nidulans* with FM4-64. Fungal Genet Biol **42:**963-975.

28. **Taheri-Talesh N, Horio T, Araujo-Bazán LD, X., Espeso EA, Peñalva MA, Osmani SA, Oakley BR.** 2008. The tip growth apparatus of *Aspergillus nidulans*. Mol Biol Cell **19:**1439-1449.

29. **Abenza JF, Pantazopoulou A, Rodríguez JM, Galindo A, Peñalva MA.** 2009. Long-distance movement of *Aspergillus nidulans* early endosomes on microtubule tracks. Traffic **10:**57-75.

30. **Pantazopoulou A, Peñalva MA.** 2009. Organization and dynamics of the *Aspergillus nidulans* Golgi during apical extension and mitosis. Mol Biol Cell **20:**4335-4347.

524 31. **Taheri-Talesh N, Xiong Y, Oakley BR.** 2012. The Functions of Myosin II and Myosin V
525 Homologs in Tip Growth and Septation in *Aspergillus nidulans*. PLoS ONE **7:**e31218.

526 32. **Valdez-Taubas J, Pelham HR.** 2003. Slow diffusion of proteins in the yeast plasma
527 membrane allows polarity to be maintained by endocytic cycling. Curr Biol. **13:**1636-1640.

528 33. **Lewis MJ, Nichols BJ, Prescianotto-Baschong C, Riezman H, Pelham HR.** 2000.
529 Specific retrieval of the exocytic SNARE Snc1p from early yeast endosomes. Mol Biol Cell
530 **11:**23-38.

531 34. **Yamashita RA, May GS.** 1998. Constitutive activation of endocytosis by mutation of
532 *myoA*, the myosin I gene of *Aspergillus nidulans* J Biol Chem **273:**14644-14648.

533 35. **Jones GW, Hooley P, Farrington SM, Shawcross SG, Iwanejko LA, Strike P.** 1999.
534 Cloning and characterisation of the *sagA* gene of *Aspergillus nidulans*: a gene which affects
535 sensitivity to DNA-damaging agents. Mol Gen Genet **261:**251-258.

536 36. **Gillingham AK, Munro S.** 2007. Identification of a guanine nucleotide exchange factor for
537 Arf3, the yeast orthologue of mammalian Arf6. PLoS ONE **2:**e842.

538 37. **Adams AE, Botstein D, Drubin DG.** 1991. Requirement of yeast fimbrin for actin
539 organization and morphogenesis *in vivo*. Nature **354:**404-408.

540 38. **Kaksonen M, Toret CP, Drubin DG.** 2005. A modular design for the clathrin- and actin-
541 mediated endocytosis machinery. Cell **123:**305-320.

542 39. **Kaksonen M, Sun Y, Drubin DG.** 2003. A pathway for association of receptors, adaptors,
543 and actin during endocytic internalization. Cell **115:**475-487.

544 40. **Kaksonen M, Toret CP, Drubin DG.** 2006. Harnessing actin dynamics for clathrin-
545 mediated endocytosis. Nat Rev Mol Cell Biol **7:**404-414.

546 41. **Peñalva MA, Arst HN, Jr.** 2004. Recent advances in the characterization of ambient pH
547 regulation of gene expression in filamentous fungi and yeasts. Annu Rev Microbiol. **58** 425-
548 451.

42. **Hervás-Aguilar A, Rodríguez JM, Tilburn J, Arst HN, Jr., Peñalva MA.** 2007. Evidence for the direct involvement of the proteasome in the proteolytic processing of the *Aspergillus nidulans* zinc finger transcription factor PacC. J Biol Chem **282:**34735-34747.

43. **Obara K, Kihara A.** 2014. Signaling events of the Rim101 pathway occur at the plasma membrane in a ubiquitination-dependent manner. Mol Cell Biol **34:**3525–3534.

44. **Subramanian S, Woolford CA, Desai JV, Lanni F, Mitchell AP.** 2012. *cis*- and *trans*-acting localization determinants of pH response regulator Rim13 in *Saccharomyces cerevisiae*. Eukaryot Cell **11:**1201-1209.

45. **Idrissi FZ, Blasco A, Espinal A, Geli MI.** 2012. Ultrastructural dynamics of proteins involved in endocytic budding. Proc Natl Acad Sci USA **109:**E2587-2594.

46. **Benedetti H, Raths S, Crausaz F, Riezman H.** 1994. The *END3* gene encodes a protein that is required for the internalization step of endocytosis and for actin cytoskeleton organization in yeast. Mol Biol Cell **5:**1023-1037.

47. **Sun Y, Martin AC, Drubin DG.** 2006. Endocytic internalization in budding yeast requires coordinated actin nucleation and myosin motor activity. Dev Cell **11:**33-46.

48. **Howard JP, Hutton JL, Olson JM, Payne GS.** 2002. Sla1p serves as the targeting signal recognition factor for NPFX(1,2)D-mediated endocytosis. J Cell Biol **157:**315-326.

49. **Wesp A, Hicke L, Palecek J, Lombardi R, Aust T, Munn AL, Riezman H.** 1997. End4p/Sla2p interacts with actin-associated proteins for endocytosis in *Saccharomyces cerevisiae*. Mol Biol Cell **8:**2291-2306.

50. **Wendland B, Emr SD.** 1998. Pan1p, yeast eps15, functions as a multivalent adaptor that coordinates protein-protein interactions essential for endocytosis. J Cell Biol **141:**71-84.

51. **Burston HE, Maldonado-Baez L, Davey M, Montpetit B, Schluter C, Wendland B, Conibear E.** 2009. Regulators of yeast endocytosis identified by systematic quantitative analysis. J Cell Biol **185:**1097-1110.

52. **Lin CH, MacGurn JA, Chu T, Stefan CJ, Emr SD.** 2008. Arrestin-related ubiquitin-ligase adaptors regulate endocytosis and protein turnover at the cell surface. Cell **135:**714-725.

53. **Nikko E, Sullivan JA, Pelham HR.** 2008. Arrestin-like proteins mediate ubiquitination and endocytosis of the yeast metal transporter Smf1. EMBO Rep. **9:**1216-1221.

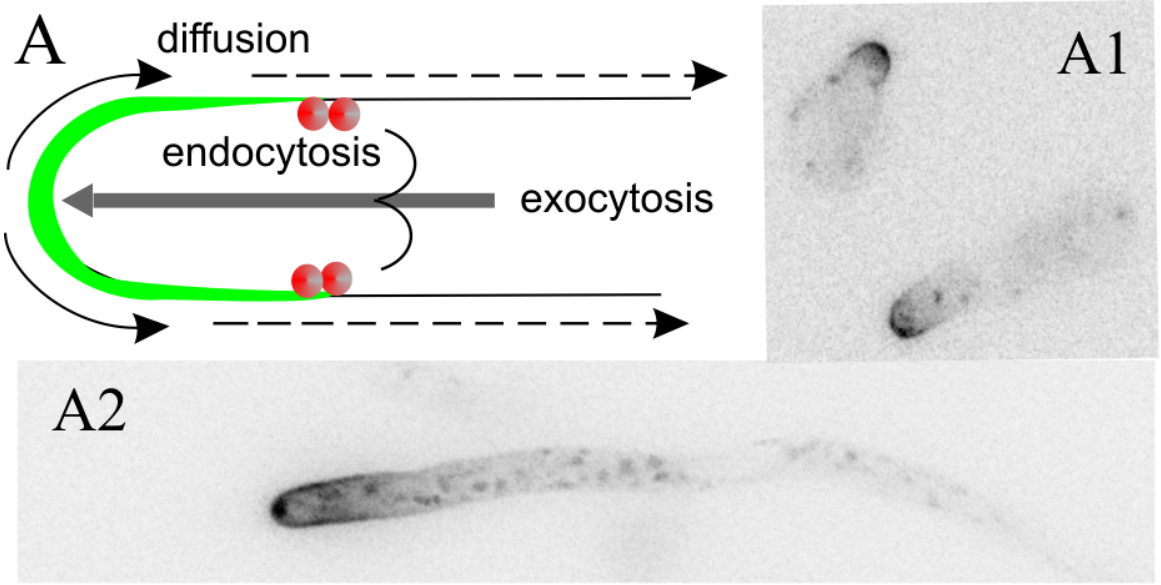
54. **Becuwe M, Vieira N, Lara D, Gomes-Rezende J, Soares-Cunha C, Casal M, Haguenauer-Tsapis R, Vincent O, Paiva S, Leon S.** 2012. A molecular switch on an arrestin-like protein relays glucose signaling to transporter endocytosis. J Cell Biol **196:**247-259.

55. **Karachaliou M, Amillis S, Evangelinos M, Kokotos AC, Yalelis V, Diallinas G.** 2013. The arrestin-like protein ArtA is essential for ubiquitination and endocytosis of the UapA transporter in response to both broad-range and specific signals. Mol Microbiol **88:**301-317.

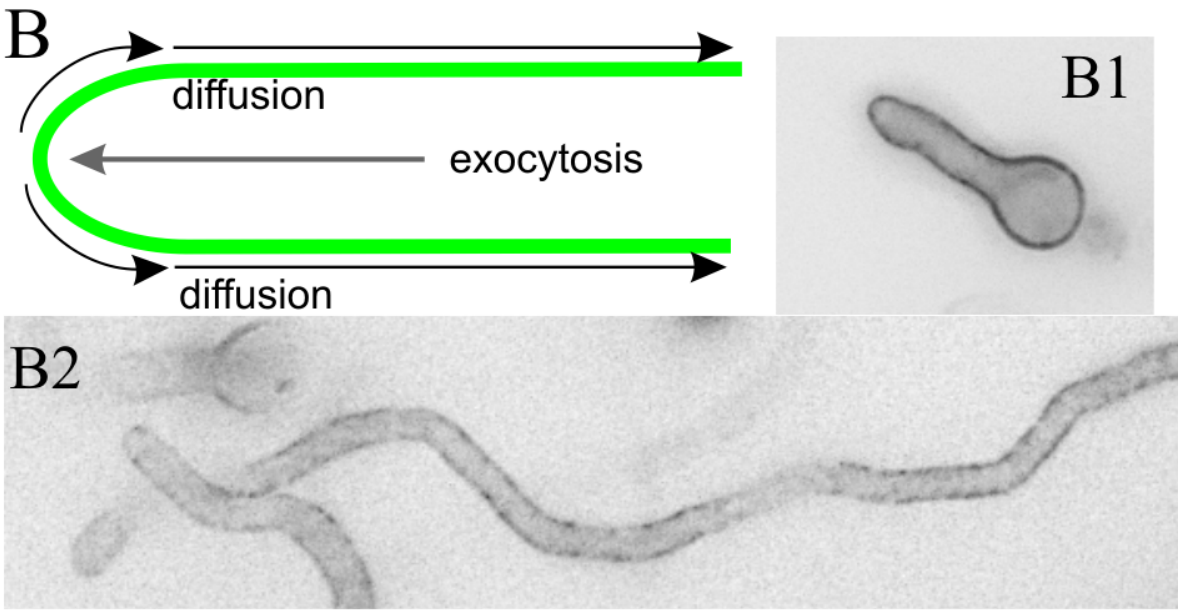
56. **Becuwe M, Leon S.** 2014. Integrated control of transporter endocytosis and recycling by the arrestin-related protein Rod1 and the ubiquitin ligase Rsp5. eLife **3**.

588 Table 1. Strains used in this work
589
590

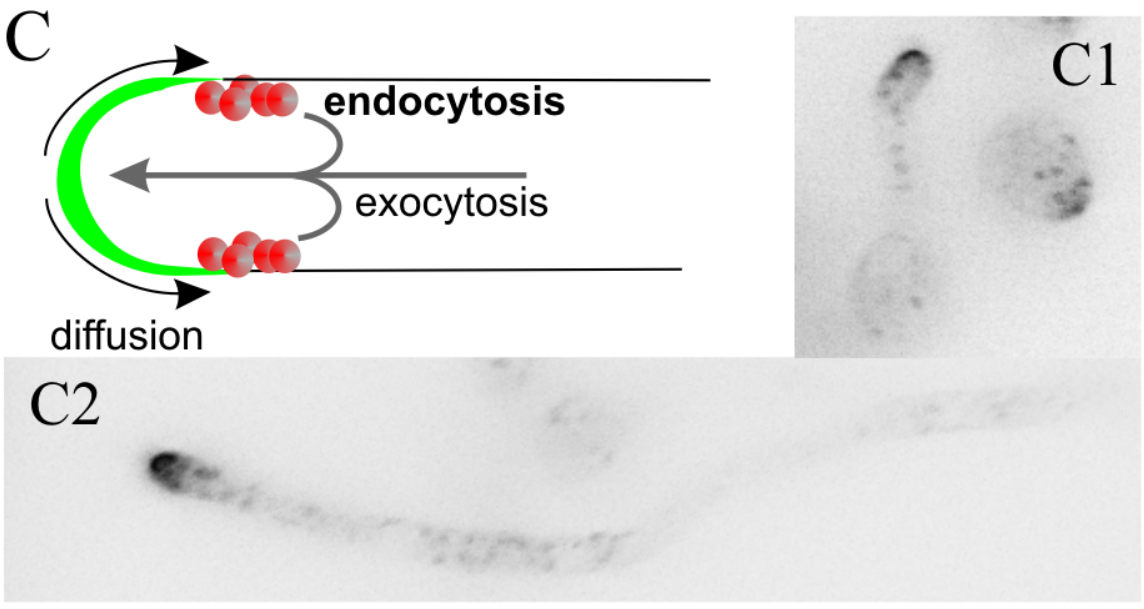
Strain Code	Genotype
MAD991	*wA*3; *pyroA*4; *myoA*^{S371E}
MAD1269	*yA*2; *inoB*2; *argB*2*::[argB*-alcAp::palB-gfp]*; *palB*38
MAD1329	*yA*2; *inoB*2; *argB*2; *palB*38
MAD1350	*pacC*900; *palH*72
MAD1362	*inoB*2; *palB*38; *pacC*900;
MAD1739	*pyrG*89; *pyroA*4; *nkuA*Δ*::bar*
MAD2335	*pyrG*89; *pyroA*4; *riboB*2; *nkuA*Δ*::argB*; *arfB::Tn::pyr*-4
MAD2384	*pyroA*4; *slaB*1; *pyrG*89; *nkuA*Δ*::bar*
MAD2467	*argB*2*::[argB*-alcAp::gfp-synA]*; *nkuA*Δ*::bar*; *pyroA*4
MAD2556	*yA*2; *pabaA*1; *pyroA*4; *gfp-synA::pyrG*^{fum}; *slaB*1; *pyrG*89*?*; *nkuA*Δ*::bar?*
MAD2560	*wA*2; *pabaA*1; *pyroA*4*::[pyroA*-gpdA*^{mini}*::palH-gfp]*
MAD2673	*gfp-synA::pyrG*^{fum}; *pyrG*89*?*; *nkuA*Δ*::bar?*
MAD2725	*slaB*1; *pyroA*4*::[gpdA*^{mini}*-palH::gfp-pyroA*]*; *nkuA*Δ*::bar?*; *pyrG*89*?*
MAD3492	*yA*2; *pabaA*1; *argB*2*::[argB*-alcAp::gfp-synA*$^{(en-)}$*]*
MAD3802	*pyroA*4; *palB-gfp::pyrG*^{fum}; *pyrG*89; *nkuA*Δ*::bar*
MaD3803	*pyroA*4; *palB-gfp::pyrG*^{fum}; *pyrG*89; *nkuA*Δ*::bar*
MAD3877	*pyroA*4; *pacC*900
MAD3964	*slaB*1; *pyrG*89; *pyroA*4; *pacC*900
MAD3968	*nkuA*Δ*::argB*; *argB*2; *pyrG*89; *pyroA*4; *riboB*2; *sagA*Δ*::riboB*^{fum}
MAD4209	*fimA::Tn431::pyr*-4; *pyrG*89; *pyroA*4; *nkuA*Δ*::argB*; *riboB*2; *veA*1
MAD4251	*pyroA*4; *fimA::Tn*341*::pyr*-4; *pyrG*89*?*; *nkuA*Δ*::argB?*; *gfp-synA::pyrG*^{fum}
MAD4269	*fimA::Tn*431*::pyr*-4; *pacC*900; *pyroA*4; *inoB*2; *pyrG*89*?*; *nkuA*Δ*::argB?*
MAD4270	*fimA::Tn*431*::pyr*-4; *pacC*900; *pyroA*4; *pyrG*89*?*; *nkuA*Δ*::argB?*
MAD4298	*wA*2; *fimA::Tn*431*::pyr*-4; *pyrG*89*?*; *nkuA*Δ*::argB?*; *pyroA*4*::[pyroA*-gpdA*^{mini}*::palH-gfp]*
MAD4384	*wA*4; *pyrG*89*?*; *inoB*2; *nkuA*Δ*::argB?*; *arfB::Tn::pyr*-4; *pacC*900
MAD4386	*pyrG*89*?*; *nkuA*Δ*::argB?*; *arfB::Tn::pyr*-4; *pyroA*4*::[pyroA*-gpdA*^{mini}*::palH-gfp]*
MAD4387	*pyrG*89*?*; *pyroA*4; *nkuA*Δ*::argB?*; *arfB::Tn::pyr*-4; *gfp-synA::pyrG*^{fum}
MAD4546	*nkuA*Δ*::argB?; pyrG*89*?; pyroA*4*::[pyroA*-gpdA*^{mini}*::palH-gfp]*; *riboB*2*?*; *sagA*Δ*::riboB*^{fum}
MAD4549	*wA*4; *nkuA*Δ*::argB; argB*2*?*; *pyrG*89*?*; *pyroA*4; *riboB*2*?*; *sagA*Δ*::riboB*^{fum}; *gfp::synA::pyrG*^{fum}
MAD4616	*wA*4; *myoA*^{S371E}; *gfp-synA::pyrG*^{fum}
MAD4618	*wA*4; *myoA*^{S371E}; *pyroA*4*::[pyroA*-gpdA*^{mini}*::palH-gfp]*
MAD4627	*wA*4; *myoA*^{S371E}; *pacC*900



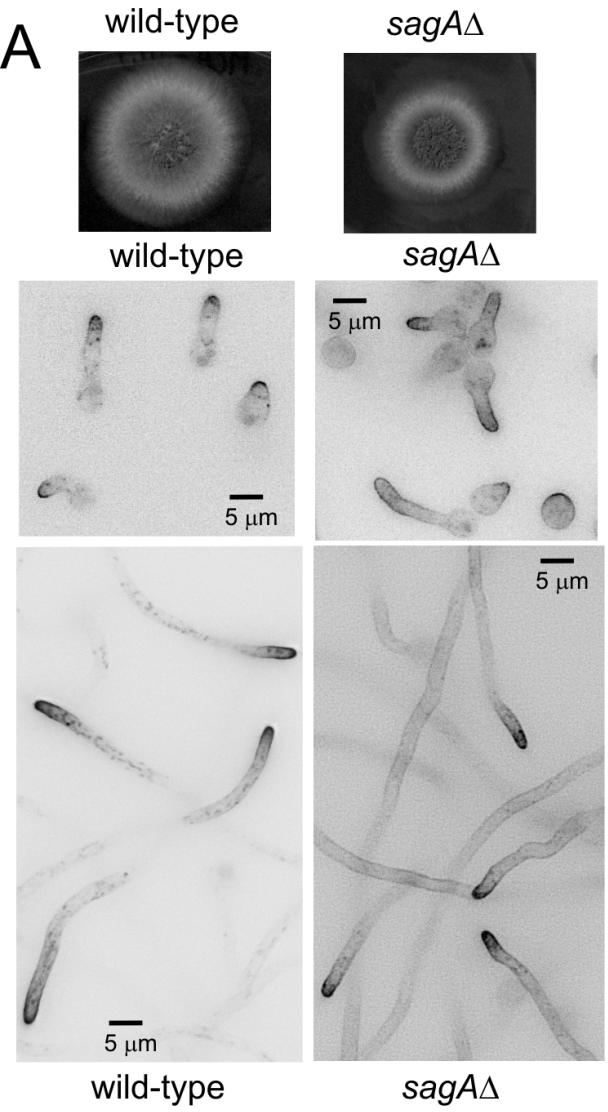
wt, SynA

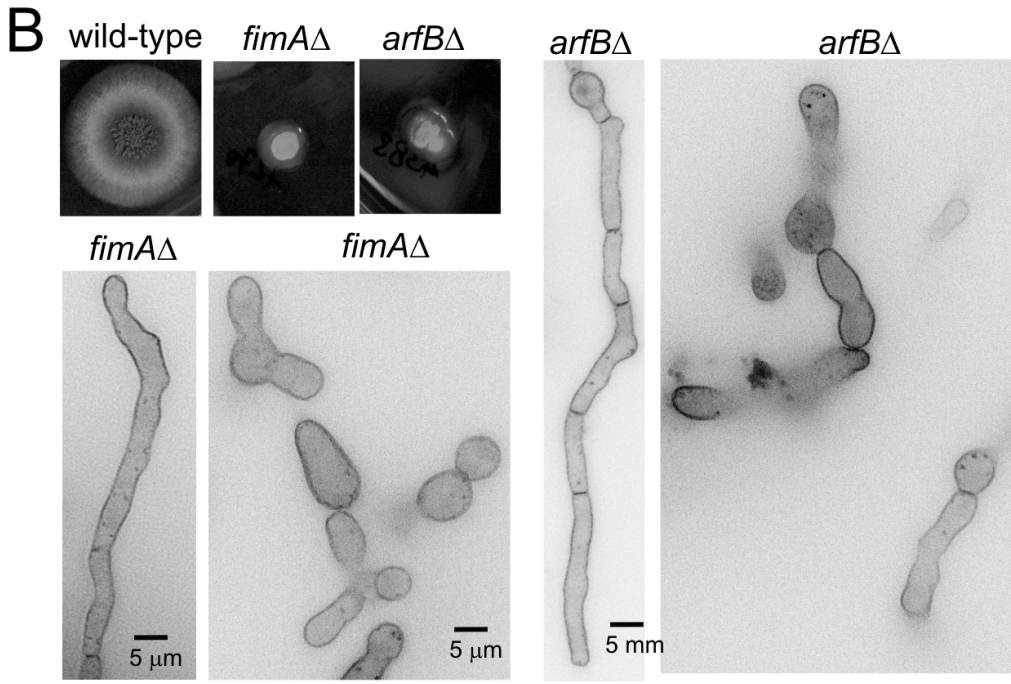


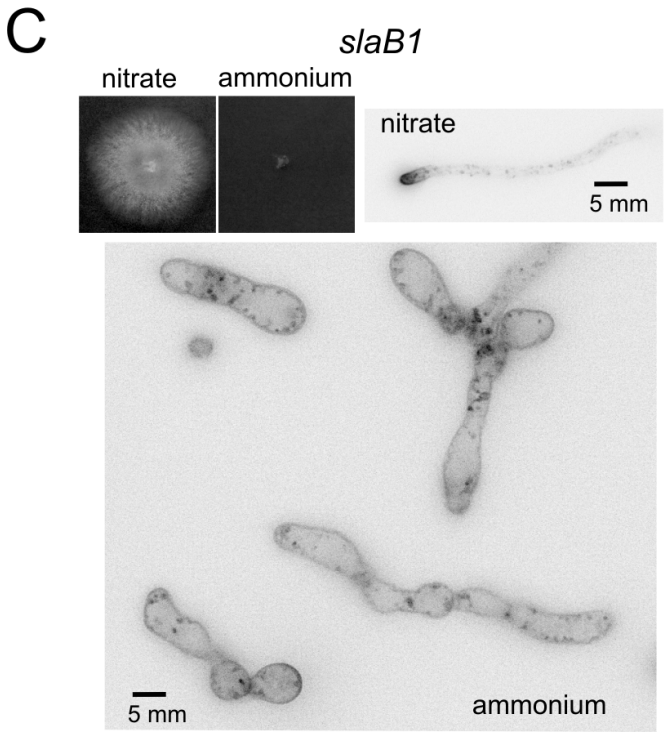
wt, SynA^{en-} (V40A, M43A)

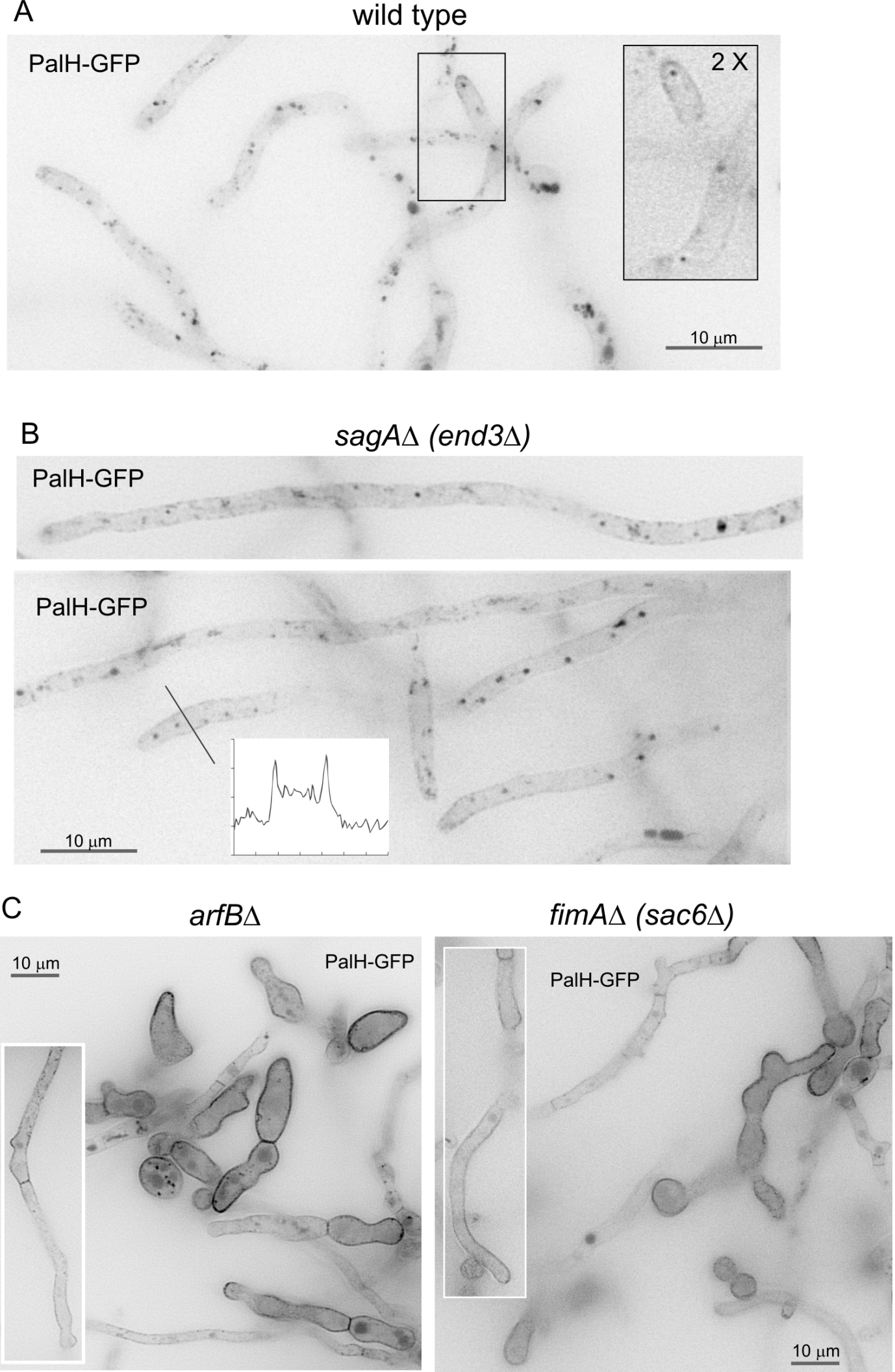


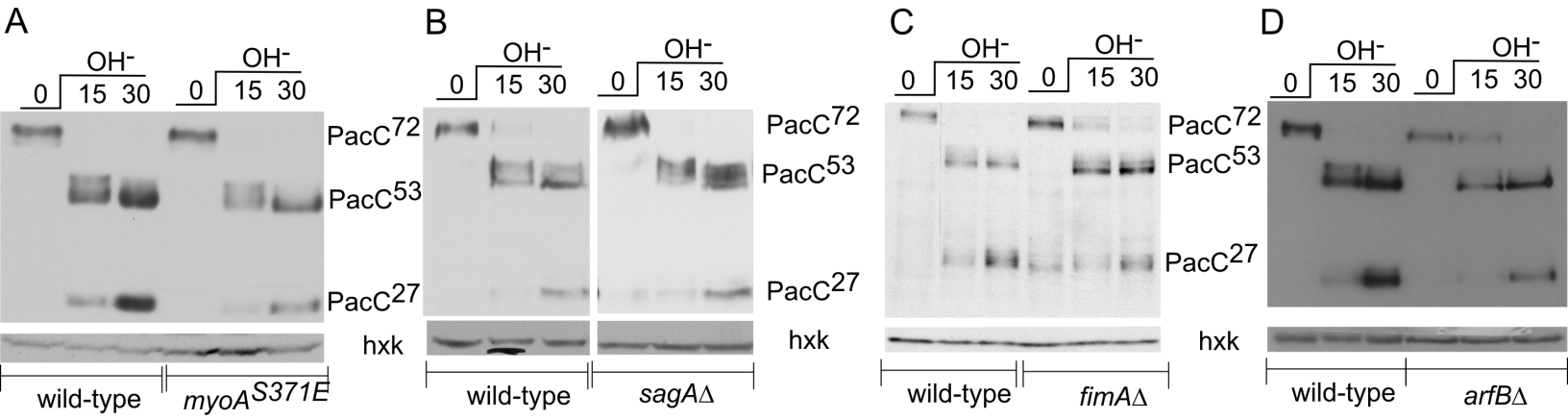
myoA^{S371E}, SynA

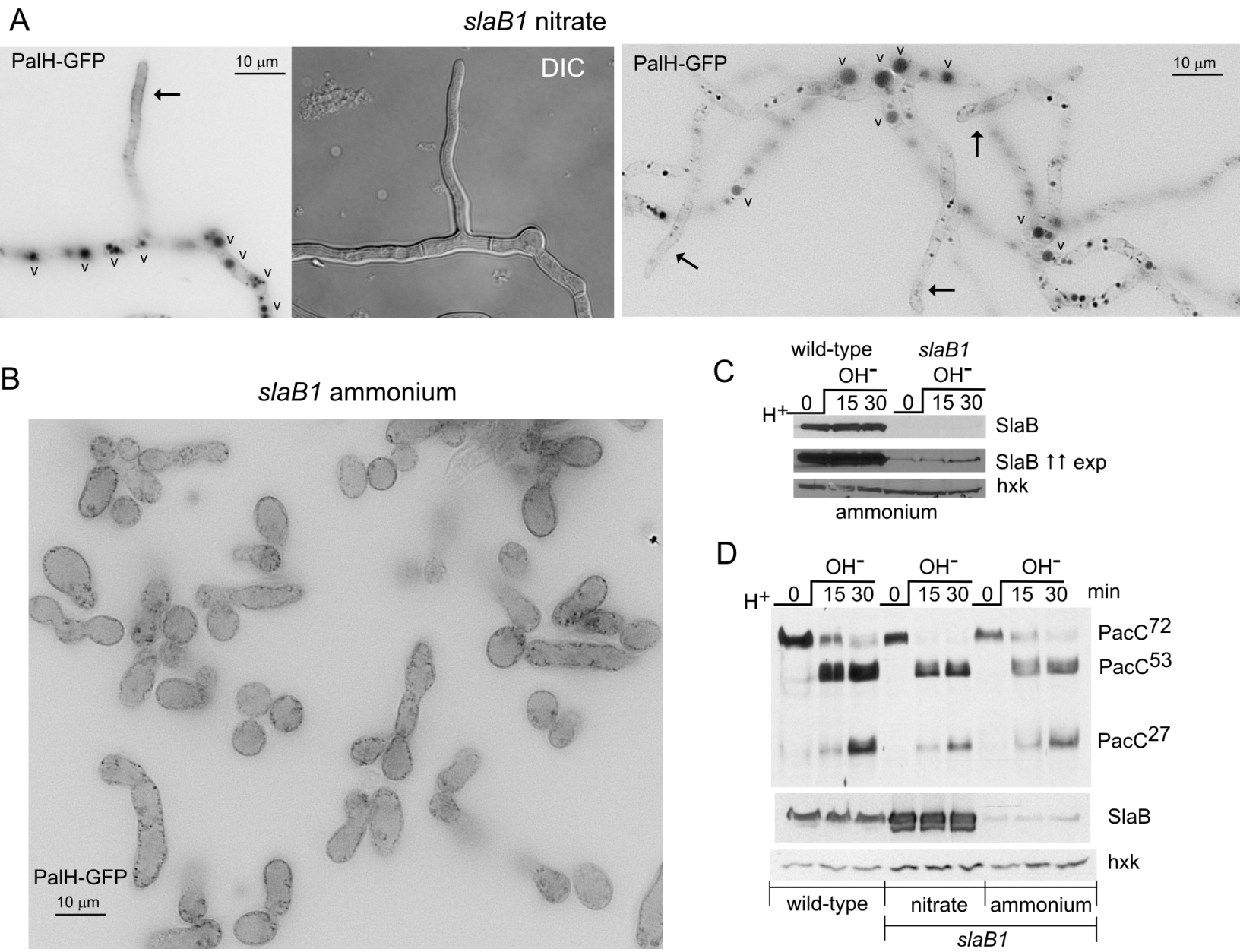

A
wild-type
sagAΔ
wild-type
sagAΔ
5 μm
5 μm
5 μm
5 μm
wild-type
sagAΔ

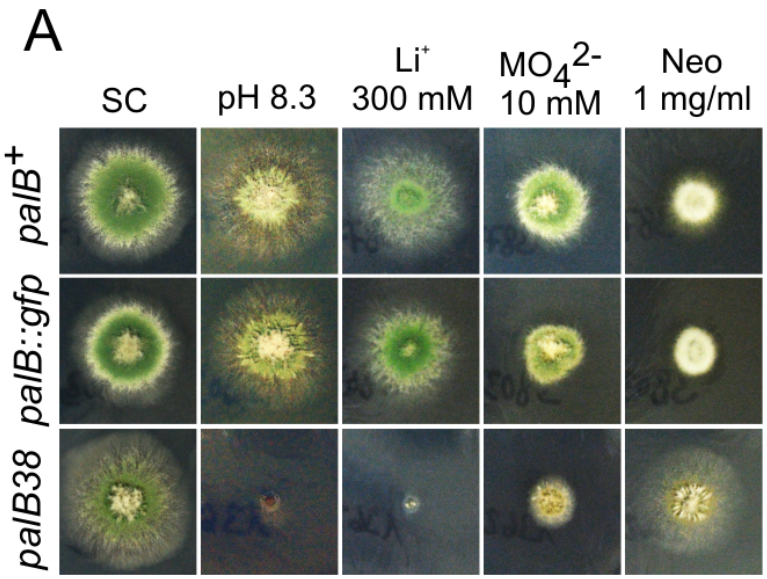

B
wild-type
fimAΔ
arfBΔ
arfBΔ
arfBΔ
fimAΔ
fimAΔ
5 μm
5 μm
5 mm

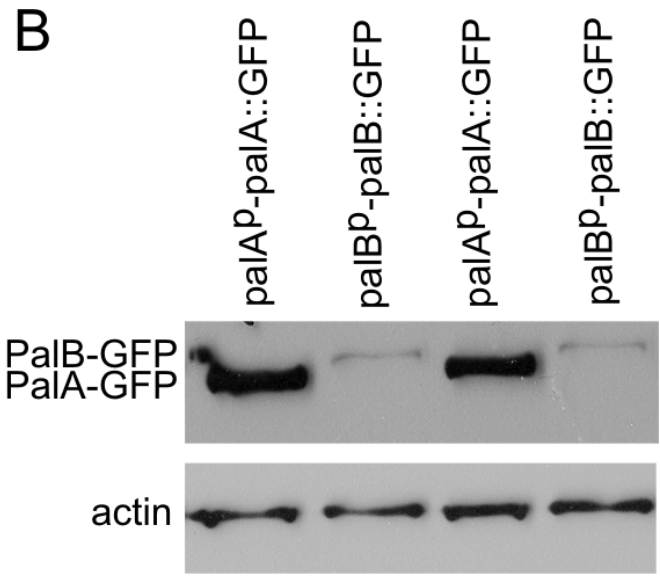

C
slaB1
nitrate
ammonium
nitrate
5 mm
5 mm
ammonium

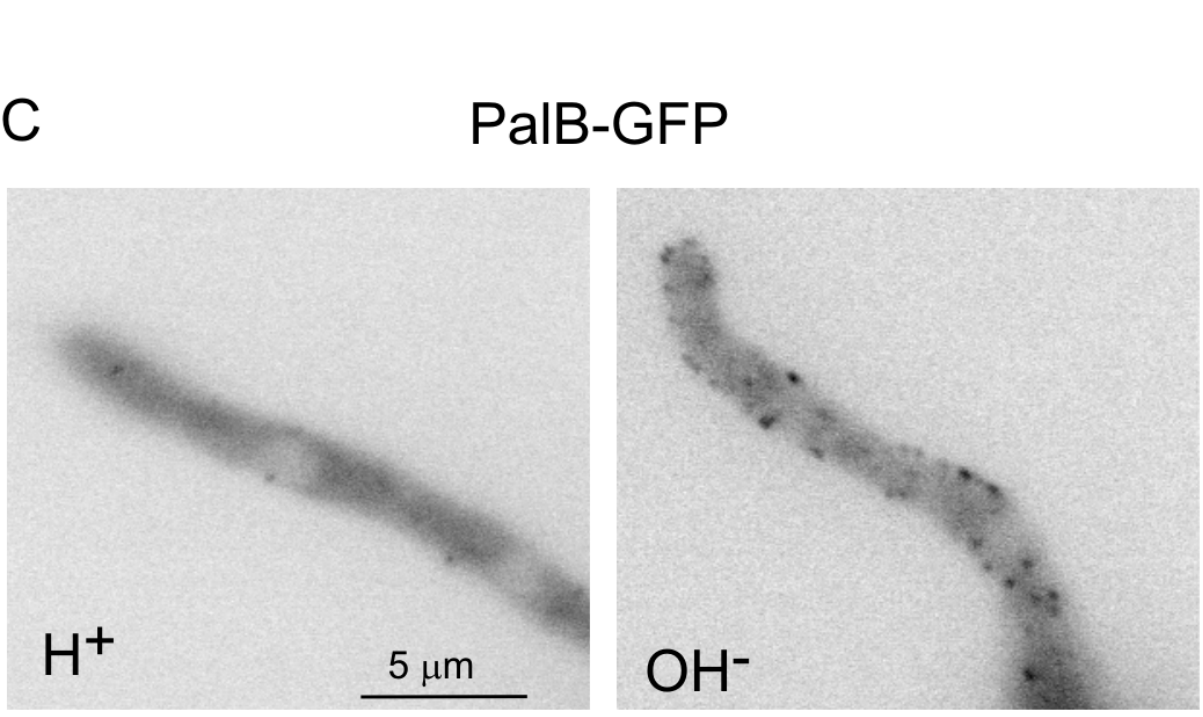

A
wild type
PalH-GFP
2 X
10 μm
B
sagAΔ (end3Δ)
PalH-GFP
PalH-GFP
10 μm
C
arfBΔ
fimAΔ (sac6Δ)
10 μm
PalH-GFP
PalH-GFP
10 μm

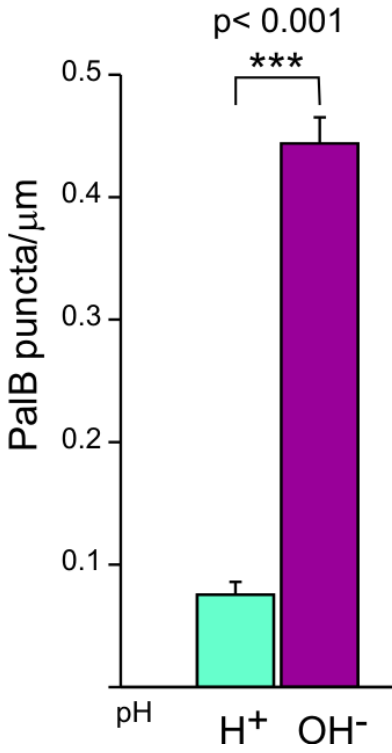

A
OH-
0 15 30
OH-
0 15 30
PacC72
PacC53
PacC27
hxk
wild-type
myoAS371E
B
OH-
0 15 30
OH-
0 15 30
PacC72
PacC53
PacC27
hxk
wild-type
sagAΔ
C
OH-
0 15 30
OH-
0 15 30
PacC72
PacC53
PacC27
hxk
wild-type
fimAΔ
D
OH-
0 15 30
OH-
0 15 30
PacC72
PacC53
PacC27
hxk
wild-type
arfBΔ


A
slaB1 nitrate
PalH-GFP
10 μm
DIC
PalH-GFP
10 μm
B
slaB1 ammonium
PalH-GFP
10 μm
C
wild-type
slaB1
OH-
OH-
H+
0
15 30
0
15 30
SlaB
SlaB ↑↑ exp
hxk
ammonium
D
OH-
OH-
OH-
H+
0
15 30
0
15 30
0
15 30
min
PacC72
PacC53
PacC27
SlaB
hxk
wild-type
nitrate
ammonium
slaB1


A
SC
pH 8.3
Li+ 300 mM
MO4 2- 10 mM
Neo 1 mg/ml
palB+
palB::gfp
palB38


B
palAp-palA::GFP
palBp-palB::GFP
palAp-palA::GFP
palBp-palB::GFP
PalB-GFP
PalA-GFP
actin


C
PalB-GFP
H+
5 μm
OH-


p< 0.001
***
PalB puncta/μm
0.5
0.4
0.3
0.2
0.1
pH
H+
OH-